

Semileptonic decays $B/B_s \rightarrow (\pi, K)(l^+l^-, l\nu, \nu\bar{\nu})$ in the perturbative QCD approach beyond the leading order

Wen-Fei Wang and Zhen-Jun Xiao*

*Department of Physics and Institute of Theoretical Physics, Nanjing Normal University,
Nanjing, Jiangsu 210023, People's Republic of China*

(Received 30 June 2012; revised manuscript received 21 October 2012; published 19 December 2012)

In this paper we first calculate the form factors of $B \rightarrow (\pi, K)$ and $B_s \rightarrow K$ transitions by employing the perturbative QCD (pQCD) factorization approach with the inclusion of the next-to-leading-order (NLO) corrections, and then we calculate the branching ratios of the corresponding semileptonic decays $B/B_s \rightarrow (\pi, K)(l^+l^-, l\nu, \nu\bar{\nu})$ (here l denotes $e, \mu, \text{ and } \tau$). Based on the numerical calculations and phenomenological analysis, we find the following results: (a) For $B \rightarrow (\pi, K)$ and $B_s \rightarrow K$ transition form factors $F_{0,+,\text{T}}(q^2)$, the NLO pQCD predictions for the values of $F_{0,+,\text{T}}(0)$ and their q^2 dependence agree well with those obtained from other methods; (b) for $\bar{B}^0 \rightarrow \pi^+l^-\bar{\nu}_l, \bar{K}^0l^+l^-$ and $B^- \rightarrow \pi^0l^-\bar{\nu}_l, K^-l^+l^-$ decay modes, the NLO pQCD predictions for their branching ratios agree very well with the measured values; (c) by comparing the pQCD predictions for $\text{Br}(\bar{B}^0 \rightarrow \pi^+l^-\bar{\nu}_l)$ with the measured decay rate, we extract out the magnitude of V_{ub} : $|V_{ub}| = (3.80_{-0.60}^{+0.66}(\text{theor}) \pm 0.13) \times 10^{-3}$; (d) we also define several ratios of the branching ratios, R_ν, R_C and $R_{N1,N2,N3}$, and present the corresponding pQCD predictions, which will be tested by LHCb and the forthcoming Super-B experiments.

 DOI: [10.1103/PhysRevD.86.114025](https://doi.org/10.1103/PhysRevD.86.114025)

PACS numbers: 13.20.He, 12.38.Bx, 14.40.Nd

I. INTRODUCTION

The semileptonic decays $B \rightarrow (\pi, K)(l^+l^-, l\bar{\nu}, \nu\bar{\nu})$ and $B_s \rightarrow K(l^+l^-, l\bar{\nu}, \nu\bar{\nu})$ with $l = (e, \mu, \tau)$ are very interesting B/B_s decays modes and play an important role in testing the standard model (SM) and in searching for the new physics (NP) beyond the SM, such as the determination of $|V_{ub}|$ and the extractions of the transition form factors $F_{0,+,\text{T}}(q^2)$ of B/B_s meson to pion and/or kaon. For the charged current $B/B_s \rightarrow Pl\bar{\nu}$ decays, the ‘‘tree’’ diagrams provide the leading-order contribution. For the neutral current $B/B_s \rightarrow Pl^+l^-$ and $P\nu\bar{\nu}$ decays, however, the leading-order SM contributions come from the photon penguin, the Z penguin, and the W^+W^- box diagrams, as shown in Fig. 1, where the symbol \oplus denotes the corresponding one-loop SM contributions.

On the experiment side, some decay modes among all the considered $B \rightarrow P(l^+l^-, l\nu, \nu\bar{\nu})$ decays have been measured by CLEO, BABAR, Belle, and LHCb experiments [1–5]. The $B_s \rightarrow K(l^+l^-, l\nu, \nu\bar{\nu})$ decays are now under study and will be measured by the LHCb and the forthcoming Super-B experiments [6,7].

On the theory side, the considered semileptonic decays strongly depend on the values and the shape of the $B/B_s \rightarrow P$ form factors. At present, there are various approaches to calculate the $B/B_s \rightarrow (\pi, K)$ transition form factors, such as the lattice QCD technique [8], the light-cone QCD sum rules (LCSRs) [9–12], as well as the perturbative QCD (pQCD) factorization approach [13–17]. The direct perturbative calculations of the one-gluon exchange diagram for the $B_{(s)}$ meson transition form factors suffer from the

end-point singularities. Because of these end-point singularities, it was claimed that the $B \rightarrow P$ transition form factors are not calculable perturbatively in QCD [18].

In the pQCD factorization approach [19], however, a form factor is generally written as the convolution of a hard amplitude with initial-state and final-state hadron distribution amplitudes. In fact, in the end-point region, the parton transverse momenta k_T is not negligible. If the large double logarithmic term $\alpha_s \ln^2(k_T)$ and large logarithms $\alpha_s \ln^2(x)$ are resummed to all orders, the relevant Sudakov form factors from both the k_T resummation and the threshold resummation [20,21] can cure the end-point singularity which makes the perturbative calculation of the hard amplitudes infrared safe, and then the main contribution comes from the perturbative regions.

In Refs. [13,16], for example, the authors calculated the $B \rightarrow \pi, \rho$ [13] and $B \rightarrow S$ form factors [16] at the leading order by employing the pQCD factorization approach and found that the values of the corresponding form factors coming from the pQCD factorization approach agree well with those obtained by using other methods [9–12]. In a recent paper [22], Li, Shen, and Wang calculated the next-to-leading-order (NLO) corrections to the $B \rightarrow \pi$ transition form factors at leading twist in the k_T factorization theorem. They found that the NLO corrections amount up to only 30% of the form factors at the large recoil region of the pion.

In this paper, based on the assumption of the $SU(3)$ flavor symmetry, we first extend the NLO results about the $B \rightarrow \pi$ form factors as presented in Ref. [22] to the cases of $B \rightarrow K$ and $B_s \rightarrow K$ directly and then calculate the q^2 dependence of the differential decay rates and the branching ratios of the considered B/B_s semileptonic decay modes and extract $|V_{ub}|$ based on our calculations.

*xiaozhenjun@njnu.edu.cn

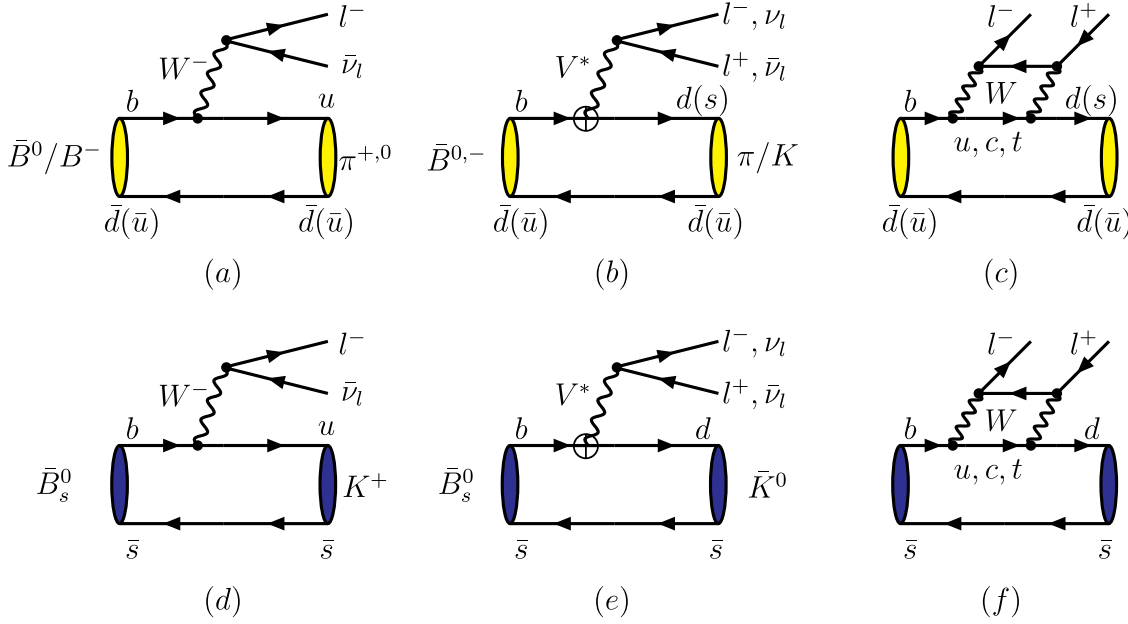


FIG. 1 (color online). The typical Feynman diagrams for the semileptonic decays $B/B_s \rightarrow (\pi, K)(l^+l^-, l\bar{\nu}, \nu\bar{\nu})$, where the symbol \oplus in (b) and (e) denotes the flavor-changing neutral current vertex with $V = \gamma$ and/or Z boson.

This paper is organized as follows. In Sec. II, we collect the distribution amplitudes of the B/B_s mesons and the π , K mesons being used in the calculation and give the k_T -dependent NLO expressions of the corresponding transition form factors. In Sec. III, based on the k_T factorization theorem, we calculate and present the expressions for the $B/B_s \rightarrow \pi, K$ transition form factors in the large recoil regions. The numerical results and relevant discussions are given in Secs. IV and V, contains the conclusions and a short summary.

II. THE THEORETICAL FRAMEWORK AND NLO CORRECTIONS

For the sake of simplicity, we use B to denote both the B and B_s meson, and P denotes final meson π or K from now on. As usual, we treat the B meson as a heavy-light system. In the B meson rest frame, the m_B stands for the mass of B meson, and we define the B meson momentum p_1 and the final meson P (say π or K meson) momentum p_2 in the light-cone coordinates

$$p_1 = \frac{m_B}{\sqrt{2}}(1, 1, 0_T), \quad p_2 = \frac{m_B}{\sqrt{2}}\eta(0, 1, 0_T), \quad (1)$$

with the energy fraction $\eta = 1 - q^2/m_B^2$ carried by the final meson (here $q = p_1 - p_2$). The light spectator momenta k_1 in the B meson and k_2 in the final meson are parametrized as

$$k_1 = \left(x_1 \frac{m_B}{\sqrt{2}}, 0, k_{1T}\right), \quad k_2 = \left(0, x_2 \eta \frac{m_B}{\sqrt{2}}, k_{2T}\right). \quad (2)$$

Because of the final pseudoscalar meson moving along the minus direction with large momentum, the plus component

of its partons momentum should be very small, so it's dropped in the expression of k_2 . But the four components of k_1 should be of the same order, i.e., $O(\bar{\Lambda})$, with $\bar{\Lambda} \equiv m_B - m_b$, m_b being the b quark mass. However, since k_2 is mainly in the minus direction with $k_2^- \sim O(m_B)$, the hard amplitudes will not depend on the minus component k_1^- as explained below. This is the reason why we do not give k_1^- in Eq. (2) explicitly.

In Ref. [22], the authors derived the k_T -dependent NLO hard kernel for the $B \rightarrow \pi$ transition form factor. We here use their results directly for $B \rightarrow \pi$ transition processes and extend the expressions of $B \rightarrow \pi$ form factors to the ones for both $B \rightarrow K$ and $B_s \rightarrow K$ transitions, under the assumption of $SU(3)$ flavor symmetry. As given in Eq. 56 of Ref. [22], the NLO hard kernel $H^{(1)}$ can be written as

$$\begin{aligned} H^{(1)} &= F(x_1, x_2, \eta, \mu_f, \mu, \zeta_1)H^{(0)} \\ &= \frac{\alpha_s(\mu_f)C_F}{4\pi} \left[\frac{21}{4} \ln \frac{\mu^2}{m_B^2} - \left(\ln \frac{m_B^2}{\zeta_1^2} + \frac{13}{2} \right) \ln \frac{\mu_f^2}{m_B^2} \right. \\ &\quad + \frac{7}{16} \ln^2(x_1 x_2) + \frac{1}{8} \ln^2 x_1 + \frac{1}{4} \ln x_1 \ln x_2 \\ &\quad + \left(2 \ln \frac{m_B^2}{\zeta_1^2} + \frac{7}{8} \ln \eta - \frac{1}{4} \right) \ln x_1 + \left(\frac{7}{8} \ln \eta - \frac{3}{2} \right) \ln x_2 \\ &\quad + \left(\frac{15}{4} - \frac{7}{16} \ln \eta \right) \ln \eta - \frac{1}{2} \ln \frac{m_B^2}{\zeta_1^2} \left(3 \ln \frac{m_B^2}{\zeta_1^2} + 2 \right) \\ &\quad \left. + \frac{101}{48} \pi^2 + \frac{219}{16} \right] H^{(0)}, \quad (3) \end{aligned}$$

where $\zeta_1 = 25m_B$ [22], μ_f is the factorization scale and set to the hard scales t_1 or t_2 as defined in the Appendix,

$\eta = 1 - (p_1 - p_2)^2/m_B^2$ is the energy fraction carried by the final meson, and finally the renormalization scale μ is defined as [22]

$$t_s(\mu_f) = \left\{ \text{Exp} \left[c_1 + \left(\ln \frac{m_B^2}{\xi_1^2} + \frac{5}{4} \right) \ln \frac{\mu_f^2}{m_B^2} x_1^{c_2} x_2^{c_3} \right]^{2/21} \mu_f \right\} \quad (4)$$

with the coefficients

$$\begin{aligned} c_1 &= -\left(\frac{15}{4} - \frac{7}{16} \ln \eta \right) \ln \eta + \frac{1}{2} \ln \frac{m_B^2}{\xi_1^2} \left(3 \ln \frac{m_B^2}{\xi_1^2} + 2 \right) \\ &\quad - \frac{101}{48} \pi^2 - \frac{219}{16}, \\ c_2 &= -\left(2 \ln \frac{m_B^2}{\xi_1^2} + \frac{7}{8} \ln \eta - \frac{1}{4} \right), \\ c_3 &= -\frac{7}{8} \ln \eta + \frac{3}{2}. \end{aligned} \quad (5)$$

In this paper, we use the distribution amplitudes (DAs) of B/B_s meson as those widely adopted in the pQCD analysis, for example, in Refs. [23–27],

$$\phi_B(x, b) = N_B x^2 (1-x)^2 \exp \left[-\frac{1}{2} \left(\frac{xm_B}{\omega_b} \right)^2 - \frac{\omega_b^2 b^2}{2} \right], \quad (6)$$

and

$$\phi_{B_s}(x, b) = N_{B_s} x^2 (1-x)^2 \exp \left[-\frac{1}{2} \left(\frac{xm_{B_s}}{\omega_{B_s}} \right)^2 - \frac{\omega_{B_s}^2 b^2}{2} \right], \quad (7)$$

where the normalization factors $N_{B(s)}$ are related to the decay constants $f_{B(s)}$ through

$$\int_0^1 dx \phi_{B(s)}(x, b=0) = \frac{f_{B(s)}}{2\sqrt{6}}. \quad (8)$$

Here the shape parameter ω_b has been fixed at 0.40 GeV by using the rich experimental data on the B mesons with $f_B = 0.21$ GeV. Correspondingly, the normalization constant N_B is 101.4. For the B_s meson, we adopt the shape parameter $\omega_{B_s} = 0.50$ GeV with $f_{B_s} = 0.23$ GeV, then the corresponding normalization constant is $N_{B_s} = 63.67$. In order to analyze the uncertainties of theoretical predictions induced by the inputs, we will vary the shape parameters ω_b and ω_{B_s} by 10%, i.e., setting $\omega_b = 0.40 \pm 0.04$ GeV and $\omega_{B_s} = 0.50 \pm 0.05$ GeV, respectively.

In Ref. [22], the authors used another form of $\phi_B(x, b)$ as given in Eq. 56 of Ref. [22] to calculate the relevant form factors, and they also investigated the effects if the popular form of $\phi_B(x, b)$ as given here in Eq. (6), i.e., the $\phi_B(x, b)$ as given in Eq. 62 of Ref. [22], was used.

For the π and K mesons, we adopt the same set of distribution amplitudes $\phi_i^A(x)$ (the leading twist-2) and $\phi_i^{P,T}(x)$ with $i = (\pi, K)$ as defined in Refs. [10,28,29]),

$$\begin{aligned} \phi_i^A(x) &= \frac{3f_i}{\sqrt{6}} x(1-x) \left[1 + a_1 C_1^{3/2}(t) + a_2 C_2^{3/2}(t) \right. \\ &\quad \left. + a_4 C_4^{3/2}(t) \right], \end{aligned} \quad (9)$$

$$\begin{aligned} \phi_i^P(x) &= \frac{f_i}{2\sqrt{6}} \left[1 + \left(30\eta_3 - \frac{5}{2} \rho_i^2 \right) C_2^{1/2}(t) \right. \\ &\quad \left. - 3 \left\{ \eta_3 \omega_3 + \frac{9}{20} \rho_i^2 (1 + 6a_2) \right\} C_4^{1/2}(t) \right], \end{aligned} \quad (10)$$

$$\begin{aligned} \phi_i^\sigma(x) &= \frac{f_i}{2\sqrt{6}} x(1-x) \left[1 + \left(5\eta_3 - \frac{1}{2} \eta_3 \omega_3 \right. \right. \\ &\quad \left. \left. - \frac{7}{20} \rho_i^2 - \frac{3}{5} \rho_i^2 a_2 \right) C_2^{3/2}(t) \right], \end{aligned} \quad (11)$$

where $t = 2x - 1$, $\rho_{\pi(K)} = m_{\pi(K)}/m_0^{\pi(K)}$ are the mass ratios (here $m_0^\pi = m_\pi^2/(m_u + m_d) = 1.4 \pm 0.1$ GeV and $m_0^K = m_K^2/(m_s + m_d) = 1.6 \pm 0.1$ GeV are the chiral mass of pion and kaon), $a_i^{\pi,K}$ are the Gegenbauer moments, and $C_n^i(t)$ are the Gegenbauer polynomials

$$\begin{aligned} C_1^{3/2}(t) &= 3t, & C_2^{1/2}(t) &= \frac{1}{2}(3t^2 - 1), \\ C_2^{3/2}(t) &= \frac{3}{2}(5t^2 - 1), & C_4^{1/2}(t) &= \frac{1}{8}(3 - 30t^2 + 35t^4), \\ C_4^{3/2}(t) &= \frac{15}{8}(1 - 14t^2 + 21t^4). \end{aligned} \quad (12)$$

The Gegenbauer moments appearing in Eqs. (9)–(11) are the following [10,28]:

$$\begin{aligned} a_1^\pi &= 0, & a_1^K &= 0.06 \pm 0.03, \\ a_2^{\pi,K} &= 0.25 \pm 0.15, & a_4^\pi &= -0.015, \\ \eta_3^{\pi,K} &= 0.015, & \omega_3^{\pi,K} &= -3. \end{aligned} \quad (13)$$

III. FORM FACTORS AND SEMILEPTONIC DECAYS

A. $B(s) \rightarrow \pi, K$ form factors

The form factors for $B \rightarrow P$ transition are defined by [30]

$$\begin{aligned} \langle P(p_2) | \bar{b}(0) \gamma_\mu q(0) | B(p_1) \rangle \\ &= \left[(p_1 + p_2)_\mu - \frac{m_B^2 - m_P^2}{q^2} q_\mu \right] F_+(q^2) \\ &\quad + \frac{m_B^2 - m_P^2}{q^2} q_\mu F_0(q^2), \end{aligned} \quad (14)$$

where $q = p_1 - p_2$ is the momentum transfer to the lepton pairs. In order to cancel the poles at $q^2 = 0$, $F_+(0)$ should be equal to $F_0(0)$. For the sake of the calculation, it is

convenient to define the auxiliary form factors $f_1(q^2)$ and $f_2(q^2)$,

$$\langle P(p_2) | \bar{b}(0) \gamma_\mu q(0) | B(p_1) \rangle = f_1(q^2) p_{1\mu} + f_2(q^2) p_{2\mu}. \quad (15)$$

in terms of $f_1(q^2)$ and $f_2(q^2)$, the form factors $F_+(q^2)$ and $F_0(q^2)$ are defined as

$$\begin{aligned} F_+(q^2) &= \frac{1}{2} [f_1(q^2) + f_2(q^2)], \\ F_0(q^2) &= \frac{1}{2} f_1(q^2) \left[1 + \frac{q^2}{m_B^2 - m_P^2} \right] \\ &\quad + \frac{1}{2} f_2(q^2) \left[1 - \frac{q^2}{m_B^2 - m_P^2} \right]. \end{aligned} \quad (16)$$

As for the tensor operator, there is only one independent form factor, which is important for the semileptonic decay,

$$\begin{aligned} \langle P(p_2) | \bar{b}(0) \sigma_{\mu\nu} q(0) | B(p_1) \rangle &= i [p_{2\mu} q_\nu - q_\mu p_{2\nu}] \\ &\quad \times \frac{2F_T(q^2)}{m_B + m_P}, \\ \langle P(p_2) | \bar{b}(0) \sigma_{\mu\nu} \gamma_5 q(0) | B(p_1) \rangle &= \epsilon_{\mu\nu\alpha\beta} p_2^\alpha q^\beta \frac{2F_T(q^2)}{m_B + m_P}. \end{aligned} \quad (17)$$

The above form factors are dominated by a single gluon exchange in the lowest order and in the large recoil regions. The factorization formula for the $B \rightarrow P$ form factors is written as [13,15]

$$\begin{aligned} \langle P(p_2) | \bar{b}(0) \gamma_\mu q(0) | B(p_1) \rangle &= g_s^2 C_F N_c \int dx_1 dx_2 d^2 k_{1T} d^2 k_{2T} \frac{dz^+ d^2 z_T}{(2\pi)^3} \frac{dy^- d^2 y_T}{(2\pi)^3} \\ &\quad \times e^{-ik_2 \cdot y} \langle P(p_2) | \bar{q}'_\gamma(y) q_\beta(0) | 0 \rangle e^{ik_1 \cdot z} \langle 0 | \bar{b}_\alpha(0) q'_\delta(z) | B(p_1) \rangle T_{H\mu}^{\gamma\beta;\alpha\delta}. \end{aligned} \quad (18)$$

In the hard-scattering kernel, the transverse momentum in the denominators is retained to regulate the end-point singularity. The masses of the light quarks and the mass difference ($\bar{\Lambda}$) between the b quark and the B meson are neglected. The terms proportional to k_{1T}^2 , k_{2T}^2 in the numerator are dropped, because they are power suppressed compared to other terms. In the transverse configuration b -space, and by including the Sudakov form factors and the threshold resummation effects, we obtain the $B \rightarrow P$ form factors as following:

$$\begin{aligned} f_1(q^2) &= 16\pi C_F m_B^2 \int dx_1 dx_2 \int b_1 db_1 b_2 db_2 \psi_B(x_1, b_1) \{ [r_0(\phi^p(x_2) - \phi^t(x_2)) \cdot h_1(x_1, x_2, b_1, b_2) \\ &\quad - r_0 x_1 \eta m_B^2 \phi^\sigma(x_2) \cdot h_2(x_1, x_2, b_1, b_2)] \cdot \alpha_s(t_1) \exp[-S_{ab}(t_1)] + [x_1(\eta \phi^a(x_2) - 2r_0 \phi^p(x_2)) \\ &\quad + 4r_0 x_1 \phi^p(x_2)] \cdot h_1(x_2, x_1, b_2, b_1) \cdot \alpha_s(t_2) \exp[-S_{ab}(t_2)] \}, \end{aligned} \quad (19)$$

$$\begin{aligned} f_2(q^2) &= 16\pi C_F m_B^2 \int dx_1 dx_2 \int b_1 db_1 b_2 db_2 \psi_B(x_1, b_1) \{ \left[\left[(x_2 \eta + 1) \phi^a(x_2) + 2r_0 \left(\frac{1}{\eta} - x_2 \right) \phi^t(x_2) - x_2 \phi^p(x_2) \right. \right. \\ &\quad \left. \left. + 3\phi^\sigma(x_2) \right] \cdot h_1(x_1, x_2, b_1, b_2) - r_0 x_1 m_B^2 (1 + x_2 \eta) \phi^\sigma(x_2) \cdot h_2(x_1, x_2, b_1, b_2) \right] \cdot \alpha_s(t_1) \exp[-S_{ab}(t_1)] \\ &\quad \left. + 2r_0 \left(\frac{x_1}{\eta} + 1 \right) \phi^p(x_2) \cdot h_1(x_2, x_1, b_2, b_1) \cdot \alpha_s(t_2) \exp[-S_{ab}(t_2)] \right\}, \end{aligned} \quad (20)$$

$$\begin{aligned} F_T(q^2) &= 8\pi C_F m_B^2 \int dx_1 dx_2 \int b_1 db_1 b_2 db_2 (1 + r_P) \psi_B(x_1, b_1) \{ \left[r_0 x_1 m_B^2 \phi^\sigma(x_2) \cdot h_2(x_1, x_2, b_1, b_2) \right. \\ &\quad \left. + \left[\phi^a(x_2) - r_0 x_2 \phi^p(x_2) + r_0 \left(\frac{2}{\eta} + x_2 \right) \phi^t(x_2) + r_0 \phi^\sigma(x_2) \right] \cdot h_1(x_1, x_2, b_1, b_2) \right] \cdot \alpha_s(t_1) \\ &\quad \left. \times \exp[-S_{ab}(t_1)] + 2r_0 \phi^p(x_2) \left(1 + \frac{x_1}{\eta} \right) \cdot h_1(x_2, x_1, b_2, b_1) \cdot \alpha_s(t_2) \exp[-S_{ab}(t_2)] \right\}, \end{aligned} \quad (21)$$

where $C_F = 4/3$ is a color factor, $r_0 = m_P^2/m_B = m_P^2/[m_B(m_q + m_{q'})]$, $r_P = m_P/m_B$, and m_P is the mass of the final pseudoscalar meson, and m_q and $m_{q'}$ is the mass of the quarks involved in the final meson. The functions h_1 and h_2 , the scales t_1 , t_2 , and the Sudakov factors S_{ab} are given in Appendix of this paper. One should note that $f_1(q^2)$, $f_2(q^2)$ and $F_T(q^2)$ as given in Eqs. (19)–(21) do not include the NLO corrections. In order to include the NLO corrections, the α_s in Eqs. (19)–(21) should be changed into $\alpha_s \cdot F(x_1, x_2, \eta, \mu_f, \mu, \zeta_1)$, where the NLO factor $F(x_1, x_2, \eta, \mu_f, \mu, \zeta_1)$ has been defined in Eq. (3).

B. Semileptonic B and B_s meson decays

For the charged current $B \rightarrow \pi l^- \bar{\nu}_l$ and $\bar{B}_s^0 \rightarrow K^+ l^- \bar{\nu}_l$ decays, as illustrated in Figs. 1(a) and 1(d) the quark-level transitions are the $b \rightarrow ul^- \bar{\nu}_l$ transitions with $l^- = (e^-, \nu^-, \tau^-)$. The effective Hamiltonian for such transitions is [31]

$$\mathcal{H}_{\text{eff}}(b \rightarrow ul\bar{\nu}_l) = \frac{G_F}{\sqrt{2}} V_{ub} \bar{u} \gamma_\mu (1 - \gamma_5) b \cdot \bar{l} \gamma^\mu (1 - \gamma_5) \nu_l, \quad (22)$$

where $G_F = 1.16637 \times 10^{-5} \text{ GeV}^{-2}$ is the Fermi-coupling constant and V_{ub} is one of the Cabbibo-Kobayashi-Maskawa (CKM) matrix elements. The corresponding differential decay widths can be written as [16,32]

$$\begin{aligned} \frac{d\Gamma(b \rightarrow ul\bar{\nu}_l)}{dq^2} &= \frac{G_F^2 |V_{ub}|^2}{192\pi^3 m_B^3} \frac{q^2 - m_l^2}{(q^2)^2} \sqrt{\frac{(q^2 - m_l^2)^2}{q^2}} \\ &\times \sqrt{\frac{(m_B^2 - m_P^2 - q^2)^2}{4q^2} - m_P^2 (m_l^2 + 2q^2)} \\ &\times [q^2 - (m_B - m_P)^2][q^2 - (m_B + m_P)^2] \\ &\times F_+^2(q^2) + 3m_l^2(m_B^2 - m_P^2)^2 F_0^2(q^2), \end{aligned} \quad (23)$$

where m_l is the mass of the lepton. If the produced lepton is e^\pm or μ^\pm , the corresponding mass terms could be neglected, and the above expression then becomes

$$\frac{d\Gamma(b \rightarrow ul\bar{\nu}_l)}{dq^2} = \frac{G_F^2}{192\pi^3 m_B^3} \lambda^{3/2}(q^2) |V_{ub}|^2 |F_+(q^2)|^2, \quad (24)$$

where $\lambda(q^2) = (m_B^2 + m_P^2 - q^2)^2 - 4m_B^2 m_P^2$ is the phase-space factor.

For those flavor-changing neutral current one-loop decay modes, such as $B \rightarrow Pl^- l^+$ with $P = (\pi, K)$ and $\bar{B}_s^0 \rightarrow \bar{K}^0 l^- l^+$ decays, as illustrated in Fig. 1, the quark-level transitions are the $b \rightarrow (s, d)l^- l^+$ transitions, and the corresponding effective Hamiltonian for such transitions is

$$\mathcal{H}_{\text{eff}} = -\frac{G_F}{\sqrt{2}} V_{tb} V_{tq}^* \sum_{i=1}^{10} C_i(\mu) O_i(\mu), \quad (25)$$

where $q = (d, s)$, $C_i(\mu)$ are the Wilson coefficients and the local operators $O_i(\mu)$ are given by [31]

$$\begin{aligned} O_1 &= (\bar{q}_\alpha c_\alpha)_{V-A} (\bar{c}_\beta b_\beta)_{V-A}, \\ O_2 &= (\bar{q}_\alpha c_\beta)_{V-A} (\bar{c}_\beta b_\alpha)_{V-A}, \\ O_3 &= (\bar{q}_\alpha b_\alpha)_{V-A} \sum_{q'} (\bar{q}'_\beta q'_\beta)_{V-A}, \\ O_4 &= (\bar{q}_\alpha b_\beta)_{V-A} \sum_{q'} (\bar{q}'_\beta q'_\alpha)_{V-A}, \\ O_5 &= (\bar{q}_\alpha b_\alpha)_{V-A} \sum_{q'} (\bar{q}'_\beta q'_\beta)_{V+A}, \\ O_6 &= (\bar{q}_\alpha b_\beta)_{V-A} \sum_{q'} (\bar{q}'_\beta q'_\alpha)_{V+A}, \\ O_7 &= \frac{em_b}{8\pi^2} \bar{q} \sigma^{\mu\nu} (1 + \gamma_5) b F_{\mu\nu}, \\ O_9 &= \frac{\alpha_{\text{em}}}{8\pi} (\bar{l} \gamma_\mu l) [\bar{q} \gamma^\mu (1 - \gamma_5) b], \\ O_{10} &= \frac{\alpha_{\text{em}}}{8\pi} (\bar{l} \gamma_\mu \gamma_5 l) [\bar{q} \gamma^\mu (1 - \gamma_5) b], \end{aligned} \quad (26)$$

where $q = (d, s)$, $q' = (u, d, c, s, b)$.

For the decays with $b \rightarrow sl^+ l^-$ transition, for example, the decay amplitude can be written as [31]

$$\begin{aligned} \mathcal{A}(b \rightarrow sl^+ l^-) &= \frac{G_F}{2\sqrt{2}} \frac{\alpha_{\text{em}}}{\pi} V_{ts}^* V_{tb} \left\{ C_{10} [\bar{s} \gamma_\mu (1 - \gamma_5) b] [\bar{l} \gamma^\mu \gamma_5 l] \right. \\ &+ C_9^{\text{eff}}(\mu) [\bar{s} \gamma_\mu (1 - \gamma_5) b] [\bar{l} \gamma^\mu l] \\ &\left. - 2m_b C_7^{\text{eff}}(\mu) \left[\bar{s} i \sigma_{\mu\nu} \frac{q^\nu}{q^2} (1 + \gamma_5) b \right] [\bar{l} \gamma^\mu l] \right\}, \end{aligned} \quad (27)$$

where $C_7^{\text{eff}}(\mu)$ and $C_9^{\text{eff}}(\mu)$ are the effective Wilson coefficients, defined as

$$C_7^{\text{eff}}(\mu) = C_7(\mu) + C'_{b \rightarrow s\gamma}(\mu), \quad (28)$$

$$C_9^{\text{eff}}(\mu) = C_9(\mu) + Y_{\text{pert}}(\hat{s}) + Y_{\text{LD}}(\hat{s}). \quad (29)$$

Here the term Y_{pert} represents the short-distance perturbative contributions and has been given in Ref. [33],

$$\begin{aligned} Y_{\text{pert}}(\hat{s}) &= h(\hat{m}_c, \hat{s}) C_0 - \frac{1}{2} h(1, \hat{s}) (4C_3 + 4C_4 + 3C_5 + C_6) \\ &- \frac{1}{2} h(0, \hat{s}) (C_3 + 3C_4) \\ &+ \frac{2}{9} (3C_3 + C_4 + 3C_5 + C_6), \end{aligned} \quad (30)$$

with $C_0 = C_1 + 3C_2 + 3C_3 + C_4 + 3C_5 + C_6$, $\hat{s} = q^2/m_B^2$, $\hat{m}_c = m_c/m_b$ and $\hat{m}_b = m_b/m_B$, while the functions $h(z, \hat{s})$ and $h(0, \hat{s})$ in the above equation are of the form

$$h(z, \hat{s}) = -\frac{8}{9} \ln \frac{m_b}{\mu} - \frac{8}{9} \ln z + \frac{8}{27} + \frac{4}{9} x - \frac{2}{9} (2+x) \sqrt{|1-x|}$$

$$\times \begin{cases} \left(\ln \left| \frac{\sqrt{1-x}+1}{\sqrt{1-x}-1} \right| - i\pi \right), & \left(x \equiv \frac{4z^2}{\hat{s}} < 1 \right), \\ 2 \arctan \frac{1}{\sqrt{x-1}}, & \left(x \equiv \frac{4z^2}{\hat{s}} > 1 \right), \end{cases} \quad (31)$$

$$h(0, \hat{s}) = \frac{8}{27} - \frac{8}{9} \ln \frac{m_b}{\mu} - \frac{4}{9} \ln \hat{s} + \frac{4}{9} i\pi. \quad (32)$$

The term $Y_{\text{LD}}(\hat{s})$ in Eq. (29) refers to the long-distance contributions from the resonant states and will be neglected because they could be excluded by experimental analysis [34,35]. The term $C'_{b \rightarrow s\gamma}$ in Eq. (28) is the absorptive part of $b \rightarrow s\gamma$ and is given by [36]

$$C'_{b \rightarrow s\gamma}(\mu) = i\alpha_s \left\{ \frac{2}{9} \eta^{14/23} [G_I(x_t) - 0.1687] - 0.03 C_2(\mu) \right\}, \quad (33)$$

with

$$G_I(x_t) = \frac{x_t(x_t^2 - 5x_t - 2)}{8(x_t - 1)^3} + \frac{3x_t^2 \ln x_t}{4(x_t - 1)^4}, \quad (34)$$

where $\eta = \alpha_s(m_W)/\alpha_s(\mu)$ and $x_t = m_t^2/m_W^2$.

The differential decay width of $b \rightarrow sl^+l^-$ is given by [16,37]

$$\frac{d\Gamma(b \rightarrow sl^+l^-)}{dq^2} = \frac{G_F^2 \alpha_{\text{em}}^2 |V_{tb}|^2 |V_{ts}^*|^2 \sqrt{\lambda(q^2)}}{512 m_B^3 \pi^5} \sqrt{\frac{q^2 - 4m_l^2}{q^2}} \frac{1}{3q^2}$$

$$\times \left[6m_l^2 |C_{10}|^2 (m_B^2 - m_P^2)^2 F_0^2(q^2) + (q^2 + 2m_l^2) \lambda(q^2) \right.$$

$$\times \left| C_9^{\text{eff}} F_+(q^2) + \frac{2C_7^{\text{eff}} (m_b - m_s) F_T(q^2)}{m_B + m_P} \right|^2$$

$$\left. + |C_{10}|^2 (q^2 - 4m_l^2) \lambda(q^2) F_+^2(q^2) \right], \quad (35)$$

where $\alpha_{\text{em}} = 1/137$ is the fine structure constant. For $b \rightarrow dl^+l^-$ decays, it is easy to derive the differential decay width from the above equation by a simple replacement, $V_{ts} \rightarrow V_{td}$ and $m_s \rightarrow m_d$.

Finally, the effective Hamiltonian for $b \rightarrow s\nu\bar{\nu}$ transition is

$$H_{b \rightarrow s\nu\bar{\nu}} = \frac{G_F}{\sqrt{2}} \frac{\alpha_{\text{em}}}{2\pi \sin^2(\theta_W)} V_{tb} V_{ts}^* \eta_X X(x_t) [\bar{s} \gamma^\mu (1 - \gamma_5) b]$$

$$\times [\bar{\nu} \gamma_\mu (1 - \gamma_5) \nu]$$

$$= C_L^{b \rightarrow s} O_L^{b \rightarrow s}, \quad (36)$$

where θ_W is the Weinberg angle with $\sin^2(\theta_W) = 0.231$, the function $X(x_t)$ can be found in Ref. [31], while $\eta_X \approx 1$

is the QCD factor [31]. The corresponding differential decay width can be written as

$$\frac{d\Gamma(b \rightarrow s\nu\bar{\nu})}{dq^2} = 3 \frac{|C_L^{b \rightarrow s}|^2 \lambda^{3/2}(m_B^2, m_P^2, q^2)}{96 m_B^3 \pi^3} |F_+(q^2)|^2. \quad (37)$$

The factor 3 in the above equation arises from the summation over the three neutrino generations. For $b \rightarrow d\nu\bar{\nu}$ transition, we can obtain the differential decay widths easily also by the simple replacements, $|V_{ts}^*| \rightarrow |V_{td}^*|$ and $m_s \rightarrow m_d$.

IV. NUMERICAL RESULTS AND DISCUSSIONS

In the numerical calculations we use the following input parameters (the masses and decay constants are all in units of GeV) [38]:

$$\Lambda_{\overline{MS}}^{(f=4)} = 0.287, \quad f_\pi = 0.13, \quad f_K = 0.16,$$

$$f_B = 0.21 \pm 0.02, \quad f_{B_s} = 0.23 \pm 0.03,$$

$$m_{B^\pm} = 5.2792, \quad m_{B^0} = 5.2795, \quad m_{B_s^0} = 5.3663,$$

$$\tau_{B^\pm} = 1.638 \text{ ps}, \quad \tau_{B^0} = 1.525 \text{ ps}, \quad \tau_{B_s^0} = 1.472 \text{ ps},$$

$$m_{\pi^\pm} = 0.1396, \quad m_{\pi^0} = 0.135, \quad m_{K^\pm} = 0.4937,$$

$$m_{K^0} = 0.4976, \quad m_\tau = 1.777, \quad m_b = 4.8,$$

$$m_W = 80.4, \quad m_t = 172. \quad (38)$$

For relevant CKM matrix elements we use $|V_{tb}| = 0.999$, $|V_{ts}| = 0.0403_{-0.0007}^{+0.0011}$, $|V_{td}/V_{ts}| = 0.211 \pm 0.001 \pm 0.005$ [38].

A. Form factors in the pQCD factorization approach

By using the definitions in Eqs. (16) and (17), and the expressions in Eqs. (19)–(21), we can calculate the values of the form factors $F_0(q^2)$, $F_+(q^2)$, and $F_T(q^2)$ for given values of q^2 in the region of $0 \leq q^2 \leq (M_B - m_P)^2$. But one should note that the pQCD predictions for the considered form factors are reliable only for small or moderate values of q^2 : say $0 \leq q^2 \leq 12 \text{ GeV}^2$. For the form factors in the larger q^2 region, one has to make an extrapolation for them from the lower q^2 region to the larger q^2 region.

For the form factor $F_0(q^2)$ of $B/B_s \rightarrow (\pi, K)$ transition, we make the extrapolation by using the pole model parametrization

$$F_0(q^2) = \frac{F_0(0)}{1 - a(q^2/m_B^2) + b(q^2/m_B^2)^2}, \quad (39)$$

where a, b are the constants to be determined by the fitting procedure. In Table I, we list the LO and NLO pQCD predictions for the form factors $F_0(0)$ and the corresponding parametrization constant a and b for $B \rightarrow (\pi, K)$ and $B_s \rightarrow K$ transitions, extracted through the fitting. The first error of $F_0(0)$ in Table I comes from the uncertainty of $\omega_B = 0.40 \pm 0.04 \text{ GeV}$ or $\omega_{B_s} = 0.50 \pm 0.05 \text{ GeV}$, the

TABLE I. The pQCD predictions for form factors $F_0(0)$ and the parametrization constant a and b for $B \rightarrow (\pi, K)$ and $B_s \rightarrow K$ transitions at the LO and NLO level, respectively.

	$F_0(0)_{\text{LO}}$	a_{LO}	b_{LO}
$B \rightarrow \pi$	$0.22^{+0.03}_{-0.02} \pm 0.03 \pm 0.01$	$0.58 \pm 0.01 \pm 0.03$	$-0.15 \pm 0.01 \pm 0.01$
$B \rightarrow K$	$0.27^{+0.04}_{-0.03} \pm 0.03 \pm 0.01$	$0.60 \pm 0.01 \pm 0.03$	$-0.15^{+0.01+0.01}_{-0.00-0.02}$
$B_s \rightarrow K$	$0.22 \pm 0.03 \pm 0.03 \pm 0.01$	$0.61 \pm 0.01^{+0.04}_{-0.03}$	$-0.16 \pm 0.00^{+0.02}_{-0.01}$
	$F_0(0)_{\text{NLO}}$	a_{NLO}	b_{NLO}
$B \rightarrow \pi$	$0.26^{+0.04}_{-0.03} \pm 0.03 \pm 0.02$	$0.50 \pm 0.01^{+0.05}_{-0.04}$	$-0.13 \pm 0.01 \pm 0.01$
$B \rightarrow K$	$0.31 \pm 0.04 \pm 0.03 \pm 0.02$	$0.53 \pm 0.01^{+0.05}_{-0.04}$	$-0.13 \pm 0.01^{+0.02}_{-0.01}$
$B_s \rightarrow K$	$0.26^{+0.04}_{-0.03} \pm 0.03 \pm 0.02$	$0.54 \pm 0.00 \pm 0.05$	$-0.15 \pm 0.01 \pm 0.01$

second error comes from the uncertainty of $f_B = 0.21 \pm 0.02$ GeV or $f_{B_s} = 0.23 \pm 0.03$ GeV, and the third one is induced by $a_1^K = 0.06 \pm 0.03$ and/or $a_2^{\pi,K} = 0.25 \pm 0.15$. The errors from the uncertainties of $m_0^\pi = 1.4 \pm 0.1$ GeV, $m_0^K = 1.6 \pm 0.1$ GeV, $|V_{ts}| = 0.0403^{+0.0011}_{-0.0007}$, and $|V_{td}/V_{ts}| = 0.211 \pm 0.001 \pm 0.005$ are very small and have been neglected.

For the form factors $F_+(q^2)$ and $F_T(q^2)$, the pole model parametrization as given in Eq. (39) does not work, and we have to use another proper parametrization method. In this paper, we use the Ball/Zwicky (BZ) parametrization method [10,39,40]. It includes the essential feature that $F_+(q^2)$ and $F_T(q^2)$ have a pole at $q^2 = m_{B^*}^2$, with $B^*(1^-)$ is a narrow resonance with $m_{B^*} = 5.325$ GeV and $m_{B_s^*} = 5.415$ GeV, which are expected to have a distinctive impact on the form factor.

For the form factors $F_+(q^2)$ and $F_T(q^2)$ of $B/B_s \rightarrow (\pi, K)$ transition, we make the extrapolation by using the BZ parametrization

$$F_i(q^2) = F_i(0) \left(\frac{1}{1 - q^2/m_{B(s)}^2} + \frac{r q^2/m_{B(s)}^2}{(1 - q^2/m_{B(s)}^2)(1 - \alpha q^2/m_{B(s)}^2)} \right), \quad (40)$$

where α and r are the shape parameters to be determined by the fitting procedure, the same as for the case of $F_0(q^2)$. In Table II, we list the pQCD predictions for the form factors $F_+(0)$, $F_T(0)$ and the corresponding shape parameters (α, r) for $B \rightarrow (\pi, K)$ and $B_s \rightarrow K$ transitions at the LO and NLO level. In Fig. 2, we show the pQCD predictions for the form factors $F_T(q^2)$ for $B \rightarrow \pi$ transition, where the dots refer to the pQCD predictions for each given value of q^2 in the large-recoil range of $0 \leq q^2 \leq 12$ GeV², while the solid curve stands for the fitted curve at the NLO level, obtained through fitting by using Eq. (40).

TABLE II. The same as in Table I, but for the pQCD predictions for the form factors $F_+(0)$, $F_T(0)$ and the corresponding shape parameters α and r at the LO and the NLO level.

	$F_+(0)_{\text{LO}}$	α_{LO}	r_{LO}
$B \rightarrow \pi$	$0.22^{+0.03}_{-0.02} \pm 0.03 \pm 0.01$	$0.61^{+0.00}_{-0.01} \pm 0.01$	$0.51 \pm 0.00 \pm 0.03$
$B \rightarrow K$	$0.27^{+0.04}_{-0.03} \pm 0.03 \pm 0.01$	$0.62^{+0.00}_{-0.01} \pm 0.01$	$0.58 \pm 0.00 \pm 0.03$
$B_s \rightarrow K$	$0.22 \pm 0.03 \pm 0.03 \pm 0.01$	$0.64 \pm 0.00 \pm 0.01$	$0.56 \pm 0.00 \pm^{+0.04}_{-0.03}$
	$F_T(0)_{\text{LO}}$	α_{LO}	r_{LO}
$B \rightarrow \pi$	$0.23 \pm 0.03 \pm 0.03 \pm 0.01$	$0.69^{+0.00}_{-0.01} \pm 0.01$	$0.55 \pm 0.01 \pm 0.03$
$B \rightarrow K$	$0.30^{+0.04}_{-0.03} \pm 0.03 \pm 0.01$	$0.71^{+0.00}_{-0.01} \pm 0.01$	$0.58 \pm 0.01 \pm 0.03$
$B_s \rightarrow K$	$0.25^{+0.04}_{-0.03} \pm 0.03 \pm 0.01$	$0.71^{+0.01}_{-0.00} \pm 0.01$	$0.59 \pm 0.00 \pm 0.03$
	$F_+(0)_{\text{NLO}}$	α_{NLO}	r_{NLO}
$B \rightarrow \pi$	$0.26^{+0.04}_{-0.03} \pm 0.03 \pm 0.02$	$0.52 \pm 0.01 \pm 0.03$	$0.45 \pm 0.00^{+0.05}_{-0.04}$
$B \rightarrow K$	$0.31 \pm 0.04 \pm 0.03 \pm 0.02$	$0.54 \pm 0.01^{+0.02}_{-0.03}$	$0.50 \pm 0.00 \pm 0.05$
$B_s \rightarrow K$	$0.26^{+0.04}_{-0.03} \pm 0.03 \pm 0.02$	$0.57 \pm 0.01 \pm 0.02$	$0.50 \pm 0.01 \pm 0.05$
	$F_T(0)_{\text{NLO}}$	α_{NLO}	r_{NLO}
$B \rightarrow \pi$	$0.26^{+0.04}_{-0.03} \pm 0.03 \pm 0.02$	$0.65^{+0.01}_{-0.02} \pm 0.01$	$0.50 \pm 0.00 \pm 0.00$
$B \rightarrow K$	$0.34^{+0.05}_{-0.04} \pm 0.03 \pm 0.02$	$0.67 \pm 0.01 \pm 0.01$	$0.53 \pm 0.00^{+0.05}_{-0.04}$
$B_s \rightarrow K$	$0.28 \pm 0.04 \pm 0.04 \pm 0.02$	$0.69 \pm 0.01 \pm 0.01$	$0.53^{+0.01+0.04}_{-0.00-0.02}$

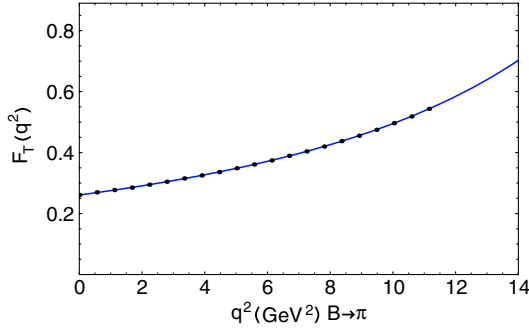


FIG. 2 (color online). The pQCD predictions for the form factors $F_T(q^2)$ for $B \rightarrow \pi$ transition, where the dots refer to the pQCD predictions for the given points of q^2 in the range of $0 \leq q^2 \leq 12 \text{ GeV}^2$, while the solid curve stands for the fitted curve at the NLO level.

In Figs. 3–5, we show the pQCD predictions for the q^2 dependence of the form factors $F_{0,+,\text{T}}(q^2)$ at the leading order (dots curves) and the next-to-leading-order (solid curve) for the considered $B \rightarrow (\pi, K)$ and $B_s \rightarrow K$ transitions, respectively. The shaded band shows the total theoretical error of the pQCD predictions, which is obtained by adding the individual theoretical errors in quadrature.

From the numerical results as listed in Table I and II and the q^2 dependence as illustrated in Figs. 3–5, one can see that

- (i) For the considered $B \rightarrow (\pi, K)$ and $B_s \rightarrow K$ transitions, the NLO pQCD predictions for the form

factors $F_{0,+,\text{T}}(0)$ agree well with the values estimated from the LCSR or other methods [10].

- (ii) $F_0(0)$ equals to $F_+(0)$ by definition, but they have different q^2 dependence, as illustrated by Figs. 3–5. We also observe the pattern of the relative strength of the form factors,

$$F_{0,+}^{B \rightarrow \pi}(0) = F_{0,+}^{B_s \rightarrow K}(0) \simeq F_{0,+}^{B \rightarrow K}(0), \quad (41)$$

$$F_{\text{T}}^{B \rightarrow \pi}(0) \simeq F_{\text{T}}^{B_s \rightarrow K}(0) \simeq F_{\text{T}}^{B \rightarrow K}(0), \quad (42)$$

which is consistent with the general expectation.

- (iii) The LO part of the form factors dominates the total contribution, while the NLO part is only around 20%. The form factor $F_0(q^2)$ has a relatively weak q^2 dependence, but $F_+(q^2)$ and $F_T(q^2)$ show a little stronger q^2 dependence when compared with $F_0(q^2)$.

As listed in Table I, our LO pQCD prediction for $F_0^{B \rightarrow \pi}(0)$ is

$$F_0^{B \rightarrow \pi}(0) = 0.22_{-0.02}^{+0.03} \pm 0.03 \pm 0.01. \quad (43)$$

Its central value is smaller than some previous LO pQCD predictions for $F_0^{B \rightarrow \pi}(0)$, for example $F_0^{B \rightarrow \pi}(0) = 0.29_{-0.05-0.01}^{+0.07+0.00}$ as given in Ref. [41]. We checked and found the following two major reasons for this difference:

- (i) We considered the contribution of the term ϕ_π^σ , which was neglected by most earlier works. At the leading order, if we neglect ϕ_π^σ term, the pQCD

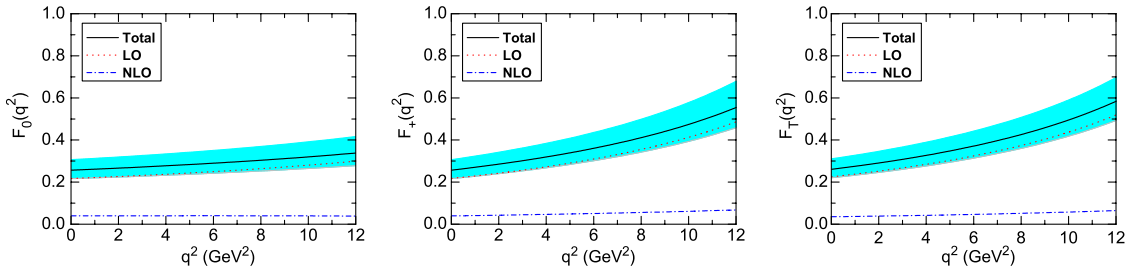


FIG. 3 (color online). The pQCD predictions for the q^2 dependence of $F_{0,+,\text{T}}(q^2)$ for $B \rightarrow \pi$ transition, where the dots curve and dot-dashed curve show the LO and NLO parts, respectively, and the solid curve stands for the total value at the NLO level, while the shaded band shows the total theoretical uncertainty.

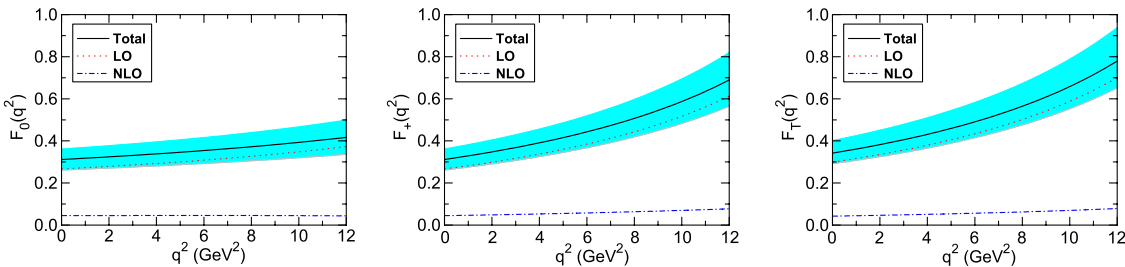
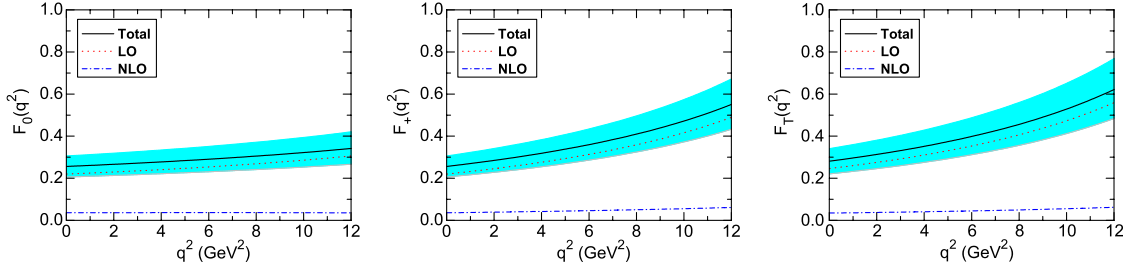


FIG. 4 (color online). The same as in Fig. 3 but for $B \rightarrow K$ transition.

FIG. 5 (color online). The same as in Fig. 3 but for $B_s \rightarrow K$ transition.

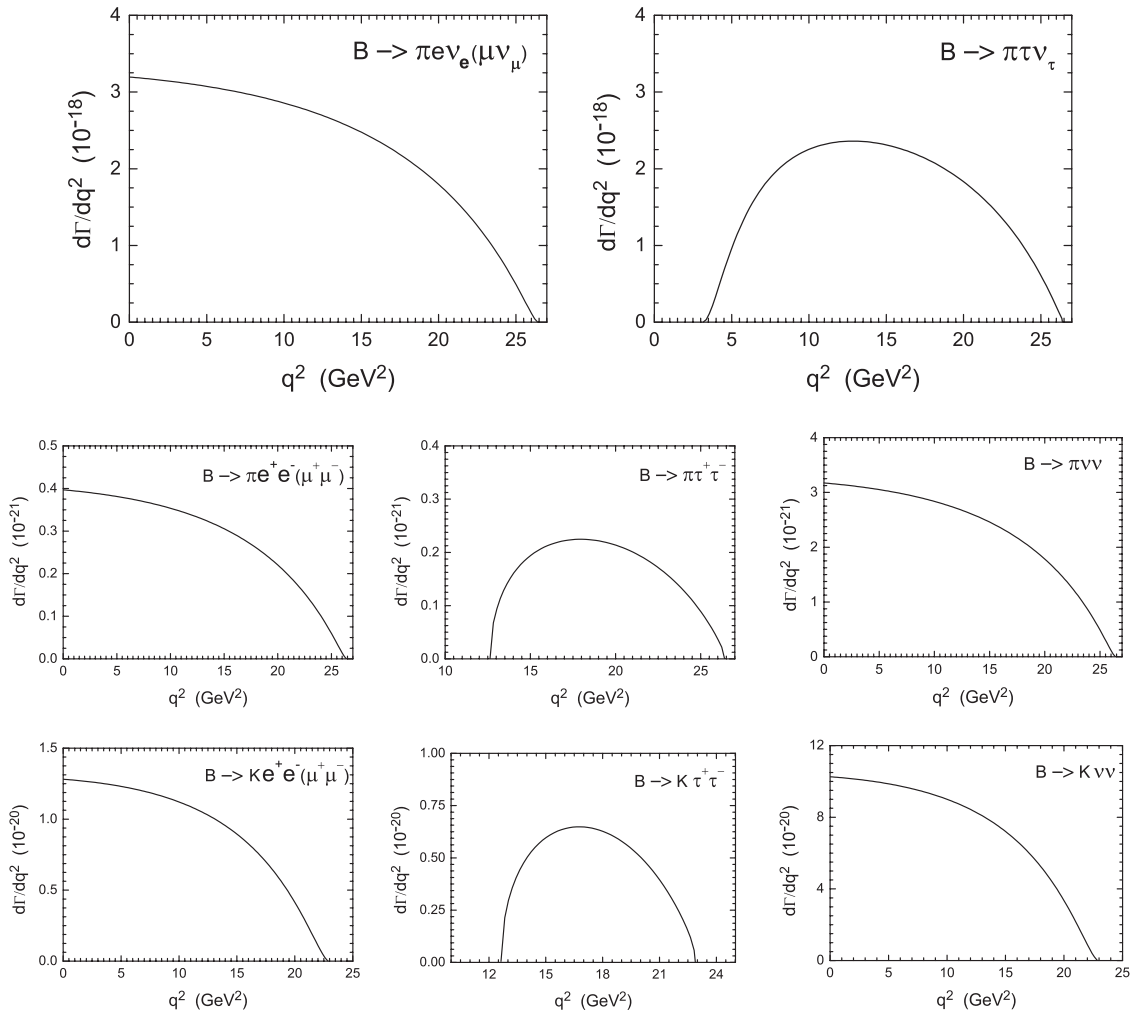
prediction for the central value of $F_0^{B \rightarrow \pi}(0)$ will be changed from 0.22 to 0.26.

- (ii) Besides the effect of the term ϕ_π^σ , if we change the value of the parameter C in the threshold resummation factor $S_l(x)$, as given in Eq. (A1), from 0.4 to 0.3 (most earlier works used $C = 0.3$), the pQCD prediction for the central value of $F_0^{B \rightarrow \pi}(0)$ will be changed further from 0.26 to 0.29, which is the value as given in Ref. [41].

- (iii) The theoretical error in our predictions is a little smaller but close to the ones given in previous works. As is well known, the estimation of the theoretical errors strongly depends on the choices of the uncertainties of relevant input parameters.

B. Decay widths and branching ratios

By using the relevant formula and the input parameters as defined or given in previous sections, it is

FIG. 6. The q^2 dependence of the differential decay rates $d\Gamma/dq^2$ for the decay processes with the $B \rightarrow \pi$ and $B \rightarrow K$ transitions.

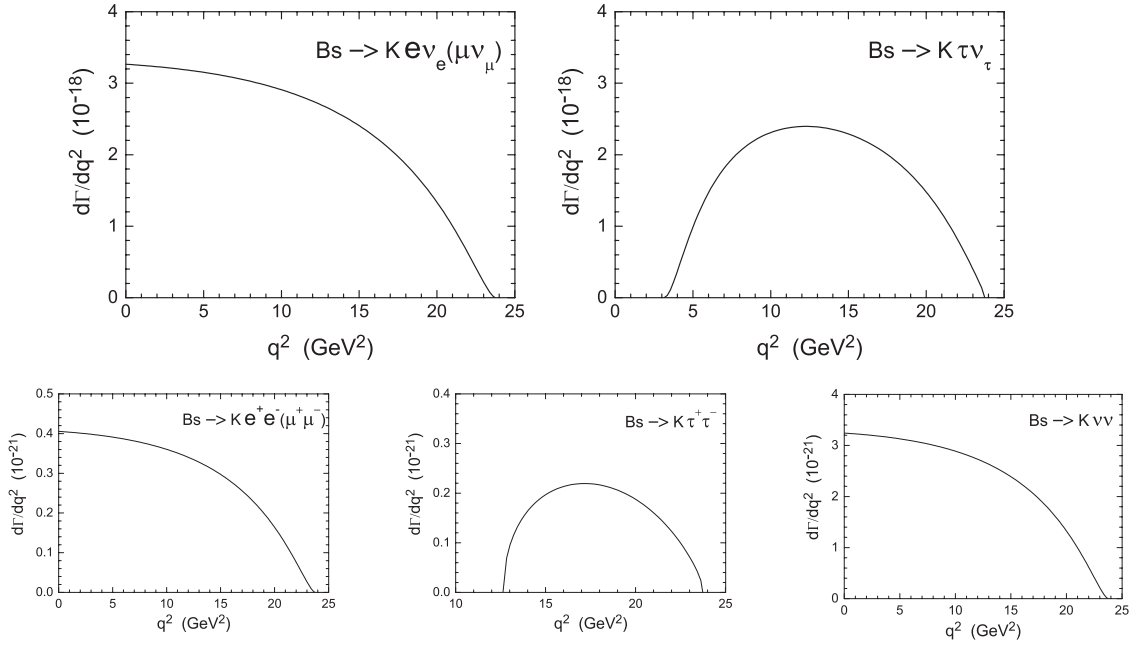


FIG. 7. The q^2 dependence of the differential decay rates $d\Gamma/dq^2$ for the decay processes with the $B_s \rightarrow K$ transitions.

straightforward to calculate the branching ratios for all the considered decays.

First, in Figs. 6 and 7, we show the differential decay rates $d\Gamma/dq^2$ for the decay modes corresponding to the $B \rightarrow (\pi, K)$ and $B_s \rightarrow K$ transitions.

By making the numerical integrations over the whole range of q^2 , we find the numerical results for the branching ratios. For the $b \rightarrow u$ charged current processes, the NLO pQCD predictions for the decay rates are the following:

$$\begin{aligned} \text{Br}(\bar{B}^0 \rightarrow \pi^+ l^- \bar{\nu}_l) &= (1.42^{+0.40}_{-0.30}(\omega_b)^{+0.28}(f_B) \pm 0.15(a_2^\pi) \\ &\pm 0.12(m_0^\pi)) \cdot \frac{|V_{ub}|^2}{|0.0038|^2} \times 10^{-4}, \end{aligned} \quad (44)$$

$$\begin{aligned} \text{Br}(\bar{B}^0 \rightarrow \pi^+ \tau^- \bar{\nu}_\tau) &= (0.90^{+0.25}_{-0.19}(\omega_b)^{+0.18}(f_B)^{+0.09}(a_2^\pi) \\ &\pm 0.08(m_0^\pi)) \cdot \frac{|V_{ub}|^2}{|0.0038|^2} \times 10^{-4}, \end{aligned} \quad (45)$$

$$\begin{aligned} \text{Br}(B^- \rightarrow \pi^0 l^- \bar{\nu}_l) &= (7.63^{+2.16}_{-1.61}(\omega_b)^{+1.52}(f_B)^{+0.82} \\ &\times (a_2^\pi)^{+0.66}(m_0^\pi)) \cdot \frac{|V_{ub}|^2}{|0.0038|^2} \times 10^{-5}, \end{aligned} \quad (46)$$

$$\begin{aligned} \text{Br}(B^- \rightarrow \pi^0 \tau^- \bar{\nu}_\tau) &= (4.85^{+1.34}_{-1.01}(\omega_b)^{+0.97}(f_B)^{+0.47} \\ &\times (a_2^\pi)^{+0.45}(m_0^\pi)) \cdot \frac{|V_{ub}|^2}{|0.0038|^2} \times 10^{-5}, \end{aligned} \quad (47)$$

$$\begin{aligned} \text{Br}(\bar{B}_s^0 \rightarrow K^+ l^- \bar{\nu}_l) &= (1.27^{+0.46}_{-0.26}(\omega_{B_s})^{+0.34}(f_{B_s})^{+0.14} \\ &\times (a_1^K)^{+0.10}(m_0^K)) \cdot \frac{|V_{ub}|^2}{|0.0038|^2} \times 10^{-4}, \end{aligned} \quad (48)$$

$$\begin{aligned} \text{Br}(\bar{B}_s^0 \rightarrow K^+ \tau^- \bar{\nu}_\tau) &= (7.78^{+2.51}_{-1.81}(\omega_{B_s})^{+2.10}(f_{B_s})^{+0.69} \\ &\times (a_1^K)^{+0.62}(m_0^K)) \cdot \frac{|V_{ub}|^2}{|0.0038|^2} \times 10^{-5}, \end{aligned} \quad (49)$$

where the first error comes from the uncertainties of $\omega_b = 0.40 \pm 0.04$ or $\omega_{B_s} = 0.50 \pm 0.05$, the second error is induced by the uncertainties of $f_B = 0.21 \pm 0.02$ or $f_{B_s} = 0.23 \pm 0.03$, the third one comes from $a_1^K = 0.06 \pm 0.03$ or $a_2^{\pi,K} = 0.25 \pm 0.15$, while the fourth one corresponds to the uncertainties of $m_0^\pi = 1.4 \pm 0.1$ GeV or $m_0^K = 1.6 \pm 0.1$ GeV.

For $\bar{B}^0 \rightarrow \pi^+ l^- \bar{\nu}_l$ and $B^- \rightarrow \pi^0 l^- \bar{\nu}_l$ decay mode, their branching ratios have been well measured by *BABAR*, *Belle*, and *CLEO* Collaborations [1–3]. The new *BABAR* measurement [1] and the new world average [42] are the following:

$$\text{Br}(\bar{B}^0 \rightarrow \pi^+ l^- \bar{\nu}_l) = \begin{cases} (1.41 \pm 0.05(\text{syst}) \pm 0.07(\text{stat})) \times 10^{-4}, & \text{BABAR}[1], \\ (1.44 \pm 0.05) \times 10^{-4}, & \text{PDG2012}[37], \end{cases} \quad (50)$$

$$\text{Br}(B^- \rightarrow \pi^0 l^- \bar{\nu}_l) = (7.78 \pm 0.28) \times 10^{-5}, \quad \text{PDG2012}[37], \quad (51)$$

On the other hand, we know that one can extract out the magnitude of the CKM matrix element V_{ub} by comparing the theoretical prediction for $\text{Br}(B \rightarrow \pi l \nu)$ with the data.

Based on the measured partial branching fraction for $B \rightarrow \pi l \nu$ in the range of $0 \leq q^2 < 12 \text{ GeV}^2$ and the most recent QCD light-cone sum-rule calculation of the form factor $F_+(q^2)$ [43], *BABAR* Collaboration found the result [1]

$$|V_{ub}| = (3.78 \pm 0.13(\text{exp})_{-0.40}^{+0.55}(\text{theor})) \times 10^{-3}, \quad (52)$$

where the two errors refer to the experimental and theoretical uncertainties.

From the differential decay rate as given in Eq. (24) and the pQCD calculation of the form factor $F_+(q^2)$ at the NLO level, we make the numerical integration over the whole range of $0 \leq q^2 \leq (M_B - m_\pi)^2$, compare the obtained branching ratio for $\bar{B}^0 \rightarrow \pi^+ l^- \bar{\nu}_l$ with the new *BABAR* measurement as given in Eq. (50) and derive our estimation for the magnitude of V_{ub} ,

$$\begin{aligned} |V_{ub}| &= (3.80_{-0.43}^{+0.50}(\omega_b)_{-0.33}^{+0.35}(f_B) \pm 0.20(a_2^\pi)_{-0.15}^{+0.16}(m_\pi^\tau) \\ &\quad \pm 0.13(\text{exp})) \times 10^{-3} \\ &= (3.80_{-0.60}^{+0.66}(\text{theor}) \pm 0.13(\text{exp})) \times 10^{-3}. \end{aligned} \quad (53)$$

The above estimation for $|V_{ub}|$ agrees well with the *BABAR* result as given in Eq. (52) [1].

Our estimation for $|V_{ub}|$ as given in Eq. (53), however, is much larger than $|V_{ub}| = (2.90_{-0.80}^{+0.77}(\text{th})_{-0.14}^{+0.13}(\text{exp})) \times 10^{-3}$ extracted in Ref. [22], where the form factors were also computed in the pQCD approach, but the B -meson distribution amplitudes as given in Eq. (59) instead of Eq. (62) (the same one as used in this paper) in Ref. [22] were used in their analysis. The major reason for the difference between the two extracted values of $|V_{ub}|$ is that different B -meson DAs were used in Ref. [22] and in our paper.

For the $B \rightarrow \pi l \bar{\nu}_l$ decay with $l = (e, \mu)$, as shown in Eq. (24), its differential decay rate is proportional to the product of the $|V_{ub}|^2$ and $|F_+(q^2)|^2$, i.e., $d\Gamma(b \rightarrow ul\bar{\nu}_l)/dq^2 \propto |V_{ub}|^2 |F_+(q^2)|^2$. As indicated also in Ref. [22], the value of the form factor $F_+(q^2)$ with the B -meson DAs in Eq. (62) of Ref. [22], which is the same one as the model in Eq. (6) of this paper, is approximately 25% smaller than those with the model in Eq. (59) of Ref. [22]. Since we use the same measured branching ratios $\text{Br}(B \rightarrow \pi l \bar{\nu}_l)$ as experimental input, a smaller form factor $F_+(q^2)$ indeed leads to a larger $|V_{ub}|$ and vice versa.

For other neutral current processes, after making the numerical integration over the whole range of $0 \leq q^2 \leq (M_B - m_\pi)^2$, we find the NLO pQCD predictions for the branching ratios. The pQCD predictions at the NLO level and currently available data are all listed in Table III. The first error of the pQCD predictions comes from the

uncertainties of ω_b or ω_{B_s} , the second error comes from the uncertainties of the f_B or f_{B_s} , the third one from a_1^K and/or $a_2^{\pi,K}$, and the fourth one is induced by the uncertainties of the chiral mass $m_0^{\pi,K}$.

From the NLO pQCD predictions for the branching ratios of all considered semileptonic decays of B and B_s meson, as listed in Eqs. (45)–(48) and Table III, we have the following points:

- (i) The branching ratios of the charged current processes $B \rightarrow \pi l \nu$ and $B_s \rightarrow K l \nu$ are all at the order of 10^{-4} . For $\bar{B}^0 \rightarrow \pi^+ l^- \bar{\nu}_l$ and $B^- \rightarrow \pi^0 l^- \bar{\nu}_l$ decay modes, the pQCD predictions for its branching ratios as shown in Eqs. (44) and (46) agree very well with the data as given in Eqs. (50) and (51). For other charged current decay modes, the pQCD predictions as given in Eqs. (45) and (47)–(49) will be tested by the LHCb and the forthcoming Super-B experiments.
- (ii) For the neutral current $\bar{B}^0 \rightarrow \bar{K}^0 l^+ l^-$ and $B^- \rightarrow K^- l^+ l^-$ decays, the NLO pQCD predictions for their branching ratios agree very well with currently available experimental measurements. For other neutral current decays, the NLO pQCD predictions are all consistent with currently available experimental upper limits and will be tested by LHCb and the forthcoming Super-B experiments.
- (iii) Because of the strong suppression of the CKM factor $|V_{td}/V_{ts}|^2 = 0.211^2$ [38], the branching ratios for the decays with $b \rightarrow d$ transitions are much smaller than those decays with the $b \rightarrow s$ transitions. Furthermore, the branching ratios of $B_{(s)} \rightarrow P \nu \bar{\nu}$ are almost an order larger than their corresponding decay modes $B_{(s)} \rightarrow P l^+ l^-$, partially due to the generation factor $N_g = 3$. In order to reduce the theoretical uncertainty of the pQCD predictions, we defined several ratios R_ν , R_C , and $R_{N1, N2, N3}$ among the branching ratios of the considered decay modes.

The NLO pQCD prediction for the ratio R_ν is of the form

$$\begin{aligned} R_\nu &= \frac{\text{Br}(\bar{B}^0 \rightarrow \pi^0 \nu \bar{\nu})}{\text{Br}(\bar{B}^0 \rightarrow \pi^0 l^+ l^-)} \approx \frac{\text{Br}(\bar{B}^0 \rightarrow \bar{K}^0 \nu \bar{\nu})}{\text{Br}(\bar{B}^0 \rightarrow \bar{K}^0 l^+ l^-)} \\ &\approx \frac{\text{Br}(B^- \rightarrow \pi^- \nu \bar{\nu})}{\text{Br}(B^- \rightarrow \pi^- l^+ l^-)} \approx \frac{\text{Br}(B^- \rightarrow K^- \nu \bar{\nu})}{\text{Br}(B^- \rightarrow K^- l^+ l^-)} \\ &\approx \frac{\text{Br}(\bar{B}_s^0 \rightarrow K^0 \nu \bar{\nu})}{\text{Br}(\bar{B}_s^0 \rightarrow K^0 l^+ l^-)} \approx 8, \end{aligned} \quad (54)$$

for $l = (e, \mu)$. These relations will be tested by experiments.

- (iv) Because of the large mass of τ lepton, we found that the considered B/B_s decays involving one or two τ 's in the final state have a smaller decay rate than those without τ . The pQCD predictions for the ratios R_C and $R_{N1, N2, N3}$ of the corresponding branching ratios of relevant decays are the following:

TABLE III. The NLO pQCD predictions for the branching ratios of the considered decays with $l = (e, \mu)$ and currently available experimental measurements [1–5,44] and the world averages [42]. The upper limits are all given at the 90% C.L.

Decay modes	NLO pQCD predictions	Data
$\text{Br}(\bar{B}^0 \rightarrow \pi^0 l^+ l^-)$	$(0.91^{+0.26+0.18}_{-0.19-0.17} \pm 0.10 \pm 0.08) \times 10^{-8}$	$< 1.2 \times 10^{-7}$
$\text{Br}(\bar{B}^0 \rightarrow \pi^0 \tau^+ \tau^-)$	$(0.28^{+0.07+0.06}_{-0.06-0.05} \pm 0.02 \pm 0.03) \times 10^{-8}$	
$\text{Br}(\bar{B}^0 \rightarrow \pi^0 \nu \bar{\nu})$	$(7.30^{+2.07+1.45+0.79+0.63}_{-1.54-1.32-0.74-0.61}) \times 10^{-8}$	$< 2.2 \times 10^{-4}$
$\text{Br}(B^- \rightarrow \pi^- l^+ l^-)$	$(1.95^{+0.55+0.39+0.21+0.17}_{-0.41-0.35-0.20-0.16}) \times 10^{-8}$	$(2.3 \pm 0.6 \pm 0.1) \times 10^{-8}$
$\text{Br}(B^- \rightarrow \pi^- \tau^+ \tau^-)$	$(0.60^{+0.16+0.12+0.04}_{-0.12-0.11-0.03} \pm 0.06) \times 10^{-8}$	
$\text{Br}(B^- \rightarrow \pi^- \nu \bar{\nu})$	$(1.57^{+0.44+0.31+0.17+0.14}_{-0.33-0.28-0.16-0.13}) \times 10^{-7}$	$< 1.0 \times 10^{-4}$
$\text{Br}(\bar{B}^0 \rightarrow \bar{K}^0 l^+ l^-)$	$(5.12^{+1.48+1.02+0.53+0.39}_{-1.10-0.93-0.51-0.38}) \times 10^{-7}$	$(4.7^{+0.6}_{-0.2}) \times 10^{-7}$
$\text{Br}(\bar{B}^0 \rightarrow \bar{K}^0 \tau^+ \tau^-)$	$(1.20^{+0.32+0.24+0.07+0.11}_{-0.25-0.22-0.07-0.10}) \times 10^{-7}$	
$\text{Br}(\bar{B}^0 \rightarrow \bar{K}^0 \nu \bar{\nu})$	$(4.11^{+1.19+0.82+0.42+0.32}_{-0.88-0.74-0.41-0.31}) \times 10^{-6}$	$< 5.6 \times 10^{-5}$
$\text{Br}(B^- \rightarrow K^- l^+ l^-)$	$(5.50^{+1.59+1.10+0.57+0.42}_{-1.18-1.00-0.55-0.41}) \times 10^{-7}$	$(5.1 \pm 0.5) \times 10^{-7}$
$\text{Br}(B^- \rightarrow K^- \tau^+ \tau^-)$	$(1.29^{+0.35+0.26}_{-0.26-0.23} \pm 0.08 \pm 0.11) \times 10^{-7}$	
$\text{Br}(B^- \rightarrow K^- \nu \bar{\nu})$	$(4.42^{+1.28+0.88+0.46+0.34}_{-0.95-0.80-0.44-0.33}) \times 10^{-6}$	$< 1.3 \times 10^{-5}$
$\text{Br}(\bar{B}_s^0 \rightarrow K^0 l^+ l^-)$	$(1.63^{+0.54+0.44+0.18+0.12}_{-0.38-0.39-0.17-0.12}) \times 10^{-8}$	
$\text{Br}(\bar{B}_s^0 \rightarrow K^0 \tau^+ \tau^-)$	$(0.43^{+0.13+0.12+0.03+0.04}_{-0.10-0.10-0.03-0.04}) \times 10^{-8}$	
$\text{Br}(\bar{B}_s^0 \rightarrow K^0 \nu \bar{\nu})$	$(1.31^{+0.43+0.35+0.14+0.10}_{-0.31-0.31-0.13-0.10}) \times 10^{-7}$	

$$R_C = \frac{\text{Br}(\bar{B}_s^0 \rightarrow P^+ l^- \bar{\nu}_l)}{\text{Br}(\bar{B}_s^0 \rightarrow P^+ \tau^- \bar{\nu}_\tau)} \approx 1.5, \quad (55)$$

$$R_{N1} = \frac{\text{Br}(\bar{B}^0 \rightarrow \pi^0 l^+ l^-)}{\text{Br}(\bar{B}^0 \rightarrow \pi^0 \tau^+ \tau^-)} \approx \frac{\text{Br}(B^- \rightarrow \pi^- l^+ l^-)}{\text{Br}(B^- \rightarrow \pi^- \tau^+ \tau^-)} \approx 3.3, \quad (56)$$

$$R_{N2} = \frac{\text{Br}(\bar{B}^0 \rightarrow \bar{K}^0 l^+ l^-)}{\text{Br}(\bar{B}^0 \rightarrow \bar{K}^0 \tau^+ \tau^-)} \approx \frac{\text{Br}(B^- \rightarrow K^- l^+ l^-)}{\text{Br}(B^- \rightarrow K^- \tau^+ \tau^-)} \approx 4.3, \quad (57)$$

$$R_{N3} = \frac{\text{Br}(\bar{B}_s^0 \rightarrow K^0 l^+ l^-)}{\text{Br}(\bar{B}_s^0 \rightarrow K^0 \tau^+ \tau^-)} \approx 3.8, \quad (58)$$

for $l = (e, \mu)$. These relations will be tested by LHCb and the forthcoming Super-B experiments.

V. SUMMARY AND CONCLUSIONS

In this paper we calculated the branching ratios of the semileptonic decays $B \rightarrow (\pi, K)(l^+ l^-, l\nu, \nu\bar{\nu})$ and $B_s \rightarrow K(l^+ l^-, l\nu, \nu\bar{\nu})$ in the pQCD factorization approach. We first evaluate the $B \rightarrow (\pi, K)$ and $B_s \rightarrow K$ transition form factors $F_{0,+T}(q^2)$ by employing the pQCD factorization approach with the inclusion of the next-to-leading-order corrections, and then we calculate the branching ratios for all considered semileptonic decays. Based on the numerical results and the phenomenological analysis, we find the following points:

- (i) For the $B \rightarrow (\pi, K)$ and $B_s \rightarrow K$ transition form factors $F_{0,+T}(q^2)$, the NLO pQCD predictions for the values of $F_{0,+T}(0)$ and their q^2 dependence agree

well with those obtained from the LCSR or other methods [9–12]. The NLO part of the form factors in the pQCD factorization approach is only around 20% of the total value.

- (ii) For the charged current $\bar{B}^0 \rightarrow \pi^+ l^- \bar{\nu}_l$ and $B^- \rightarrow \pi^0 l^- \bar{\nu}_l$ decays and the neutral current $\bar{B}^0 \rightarrow \bar{K}^0 l^+ l^-$ and $B^- \rightarrow K^- l^+ l^-$ decays, the NLO pQCD predictions for their branching ratios agree very well with the measured values.
- (iii) By comparing the pQCD predictions for $\text{Br}(\bar{B}^0 \rightarrow \pi^+ l^- \bar{\nu}_l)$ with the measured decay rate, we extract out the magnitude of the CKM element V_{ub} : $|V_{ub}| = (3.80^{+0.66}_{-0.60}(\text{theor}) \pm 0.13) \times 10^{-3}$.
- (iv) We also define several ratios of the branching ratios R_ν , R_C , and $R_{N1,N2,N3}$, and presented the corresponding pQCD predictions, which will be tested by LHCb and the forthcoming Super-B experiments.

ACKNOWLEDGMENTS

The authors would like to thank H. n. Li, Y. M. Wang, C. D. Lu, and Y. L. Shen for valuable discussions. This work is supported in part by the National Natural Science Foundation of China under Grants No. 10975074, No. 10735080, and No. 11235005.

APPENDIX A: RELATED FUNCTIONS DEFINED IN THE TEXT

In this appendix, we present the functions needed in the pQCD calculation. The threshold resummation factors $S_i(x)$ are adopted from Ref. [13],

$$S_t = \frac{2^{1+2c}\Gamma(3/2+c)}{\sqrt{\pi}\Gamma(1+c)} [x(1-x)]^c, \quad (\text{A1})$$

and we here set the parameter $c = 0.4$. The hard functions h_1 and h_2 come from the Fourier transform and can be written as [45]

$$\begin{aligned} h_1(x_1, x_2, b_1, b_2) &= K_0(\sqrt{x_1 x_2} \eta m_B b_1) [\theta(b_1 - b_2) \\ &\quad \times I_0(\sqrt{x_2} \eta m_B b_2) K_0(\sqrt{x_2} \eta m_B b_1) \\ &\quad + \theta(b_2 - b_1) I_0(\sqrt{x_2} \eta m_B b_1) \\ &\quad \times K_0(\sqrt{x_2} \eta m_B b_2)] S_t(x_2), \end{aligned} \quad (\text{A2})$$

$$\begin{aligned} h_2(x_1, x_2, b_1, b_2) &= \frac{b_1 K_1(\sqrt{x_1 x_2} \eta m_B b_1)}{2\sqrt{x_1 x_2} \eta m_B} [\theta(b_1 - b_2) \\ &\quad \times I_0(\sqrt{x_2} \eta m_B b_2) K_0(\sqrt{x_2} \eta m_B b_1) \\ &\quad + \theta(b_2 - b_1) I_0(\sqrt{x_2} \eta m_B b_1) \\ &\quad \times K_0(\sqrt{x_2} \eta m_B b_2)] S_t(x_2), \end{aligned} \quad (\text{A3})$$

where J_0 is the Bessel function and K_0, K_1, I_0 are modified Bessel functions.

The factor $\exp[-S_{ab}(t)]$ contains the Sudakov logarithmic corrections and the renormalization group evolution effects of both the wave functions and the hard-scattering amplitude with $S_{ab}(t) = S_B(t) + S_P(t)$, where

$$S_B(t) = s\left(x_1 \frac{m_B}{\sqrt{2}}, b_1\right) + \frac{5}{3} \int_{1/b_1}^t \frac{d\bar{\mu}}{\bar{\mu}} \gamma_q(\alpha_s(\bar{\mu})), \quad (\text{A4})$$

$$\begin{aligned} S_P(t) &= s\left(x_2 \frac{m_B}{\sqrt{2}}, b_2\right) + s\left((1-x_2) \frac{m_B}{\sqrt{2}}, b_2\right) \\ &\quad + 2 \int_{1/b_2}^t \frac{d\bar{\mu}}{\bar{\mu}} \gamma_q(\alpha_s(\bar{\mu})), \end{aligned} \quad (\text{A5})$$

with the quark anomalous dimension $\gamma_q = -\alpha_s/\pi$. The functions $s(Q, b)$ are defined by [13]

$$\begin{aligned} s(Q, b) &= \frac{A^{(1)}}{2\beta_1} \hat{q} \ln\left(\frac{\hat{q}}{\hat{b}}\right) - \frac{A^{(1)}}{2\beta_1} (\hat{q} - \hat{b}) + \frac{A^{(2)}}{4\beta_1^2} \left(\frac{\hat{q}}{\hat{b}} - 1\right) \\ &\quad - \left[\frac{A^{(2)}}{4\beta_1^2} - \frac{A^{(1)}}{4\beta_1} \ln\left(\frac{e^{2\gamma_E} - 1}{2}\right) \right] \ln\left(\frac{\hat{q}}{\hat{b}}\right) \\ &\quad + \frac{A^{(1)}\beta_2}{4\beta_1^3} \hat{q} \left[\frac{\ln(2\hat{q}) + 1}{\hat{q}} - \frac{\ln(2\hat{b}) + 1}{\hat{b}} \right] \\ &\quad + \frac{A^{(1)}\beta_2}{8\beta_1^3} [\ln^2(2\hat{q}) - \ln^2(2\hat{b})], \end{aligned} \quad (\text{A6})$$

where the variables are defined by $\hat{q} = \ln[Q/(\sqrt{2}\Lambda)]$, $\hat{b} = \ln[1/(b\Lambda)]$, and the coefficients $A^{(i)}$ and β_i are

$$\begin{aligned} \beta_1 &= \frac{33 - 2n_f}{12}, \quad \beta_2 = \frac{153 - 19n_f}{24}, \quad A^{(1)} = \frac{4}{3}, \\ A^{(2)} &= \frac{67}{9} - \frac{\pi^2}{3} - \frac{10n_f}{27} + \frac{8}{3}\beta_1 \ln(e^{\gamma_E}/2). \end{aligned} \quad (\text{A7})$$

Here, n_f is the number of the quark flavors, and the γ_E is the Euler constant. The hard scales t_i in the equations of this work are chosen as the largest scale of the virtuality of the internal particles in the hard b -quark decay diagram,

$$\begin{aligned} t_1 &= \max\{\sqrt{x_2} \eta m_B, 1/b_1, 1/b_2\}, \\ t_2 &= \max\{\sqrt{x_1} \eta m_B, 1/b_1, 1/b_2\}. \end{aligned} \quad (\text{A8})$$

-
- [1] P. del Amo Sanchez *et al.* (BABAR Collaboration), *Phys. Rev. D* **83**, 032007 (2011); **83**, 052011 (2011).
[2] N. E. Adam *et al.* (CLEO Collaboration), *Phys. Rev. Lett.* **99**, 041802 (2007).
[3] T. Hokuue *et al.* (Belle Collaboration), *Phys. Lett. B* **648**, 139 (2007).
[4] J. P. Lees *et al.* (BABAR Collaboration), *Phys. Rev. D* **86**, 032012 (2012); P. del Amo Sanchez *et al.* (BABAR Collaboration), *Phys. Rev. D* **82**, 112002 (2010).
[5] R. Aaij *et al.* (LHCb Collaboration), [arXiv:1210.2645](https://arxiv.org/abs/1210.2645).
[6] G. Dissertori, [arXiv:1205.2209](https://arxiv.org/abs/1205.2209).
[7] A. J. Buras and J. Girrbach, *Acta Phys. Pol. B* **43**, 1427 (2012).
[8] E. Gulez, A. Gray, M. Wingate, C. T. H. Davies, G. P. Lepage, and J. Shigemitsu, *Phys. Rev. D* **73**, 074502 (2006); **75**, 119906(E) (2007), and references therein.
[9] P. Ball, *J. High Energy Phys.* **09** (1998) 005; P. Ball and R. Zwicky, *J. High Energy Phys.* **10** (2001) 019.
[10] P. Ball and R. Zwicky, *Phys. Rev. D* **71**, 014015 (2005).
[11] G. Duplancic, A. Khodjamirian, T. Mannel, B. Melic, and N. Offen, *J. High Energy Phys.* **04** (2008) 014.
[12] A. Khodjamirian, T. Mannel, N. Offen, and Y.-M. Wang, *Phys. Rev. D* **83**, 094031 (2011).
[13] T. Kurimoto, H. N. Li, and A. I. Sanda, *Phys. Rev. D* **65**, 014007 (2001).
[14] Z. T. Wei and M. Z. Yang, *Nucl. Phys.* **B642**, 263 (2002).
[15] C. D. Lu and M. Z. Yang, *Eur. Phys. J. C* **23**, 275 (2002); **28**, 515 (2003).
[16] R. H. Li, C. D. Lu, W. Wang, and X. X. Wang, *Phys. Rev. D* **79**, 014013 (2009).
[17] T. Huang and X. G. Wu, *Phys. Rev. D* **71**, 034018 (2005).
[18] T. Huang and C. W. Luo, *Commun. Theor. Phys.* **22**, 473 (1994); A. Khodjamirian, R. Ruckl, and C. W. Winhart, *Phys. Rev. D* **58**, 054013 (1998).

- [19] T. W. Yeh and H. N. Li, *Phys. Rev. D* **56**, 1615 (1997); H. N. Li and H. L. Yu, *Phys. Rev. Lett.* **74**, 4388 (1995); *Phys. Lett. B* **353**, 301 (1995); *Phys. Rev. D* **53**, 2480 (1996).
- [20] G. Sterman, *Phys. Lett. B* **179**, 281 (1986); *Nucl. Phys.* **B281**, 310 (1987); S. Catani and L. Trentadue, *Nucl. Phys.* **B327**, 323 (1989); **B353**, 183 (1991).
- [21] H. N. Li, *Phys. Rev. D* **66**, 094010 (2002).
- [22] H. N. Li, Y. L. Shen, and Y. M. Wang, *Phys. Rev. D* **85**, 074004 (2012).
- [23] Z. J. Xiao, Z. Q. Zhang, X. Liu, and L. B. Guo, *Phys. Rev. D* **78**, 114001 (2008); Z. J. Xiao, W. F. Wang, and Y. Y. Fan, *Phys. Rev. D* **85**, 094003 (2012); X. Liu and Z. J. Xiao, *Phys. Rev. D* **86**, 074016 (2012).
- [24] Y. Y. Keum, H. N. Li, and A. I. Sanda, *Phys. Lett. B* **504**, 6 (2001); *Phys. Rev. D* **63**, 054008 (2001); C. D. Lü, K. Ukai, and M. Z. Yang, *Phys. Rev. D* **63**, 074009 (2001).
- [25] X. Liu, H. S. Wang, Z. J. Xiao, L. B. Guo, and C. D. Lü, *Phys. Rev. D* **73**, 074002 (2006); H. S. Wang, X. Liu, Z. J. Xiao, L. B. Guo, and C. D. Lü, *Nucl. Phys.* **B738**, 243 (2006).
- [26] Z. J. Xiao, D. Q. Guo, and X. F. Chen, *Phys. Rev. D* **75**, 014018 (2007); D. Q. Guo, X. F. Chen, and Z. J. Xiao, *Phys. Rev. D* **75**, 054033 (2007); X. F. Chen, D. Q. Guo, and Z. J. Xiao, *Eur. Phys. J. C* **50**, 363 (2007).
- [27] A. Ali, G. Kramer, Y. Li, C. D. Lü, Y. L. Shen, W. Wang, and Y. M. Wang, *Phys. Rev. D* **76**, 074018 (2007).
- [28] P. Ball, V. M. Braun, and A. Lenz, *J. High Energy Phys.* **05** (2006) 004.
- [29] P. Ball, *J. High Energy Phys.* **01** (1999) 010.
- [30] M. Beneke and Th. Feldmann, *Nucl. Phys.* **B592**, 3 (2001).
- [31] A. J. Buras, M. Misiak, M. Munz, and S. Pokorski, *Nucl. Phys.* **B424**, 374 (1994); G. Buchalla, A. J. Buras, and M. E. Lautenbacher, *Rev. Mod. Phys.* **68**, 1125 (1996).
- [32] P. Colangelo, F. De Fazio, R. Ferrandes, and T. N. Pham, *Phys. Rev. D* **73**, 115006 (2006).
- [33] A. J. Buras and M. Munz, *Phys. Rev. D* **52**, 186 (1995).
- [34] T. Aaltonen *et al.* (CDF Collaboration), *Phys. Rev. Lett.* **106**, 161801 (2011).
- [35] M. Beneke, G. Buchalla, M. Neubert, and C. T. Sachrajda, *Eur. Phys. J. C* **61**, 439 (2009); M. Bartsch, M. Beylich, G. Buchalla, and D. N. Gao, *J. High Energy Phys.* **11** (2009) 011.
- [36] C. H. Chen and C. Q. Geng, *Phys. Rev. D* **64**, 074001 (2001).
- [37] P. Colangelo, F. De Fazio, and W. Wang, *Phys. Rev. D* **81**, 074001 (2010).
- [38] K. Nakamura *et al.* (Particle Data Group), *J. Phys. G* **37**, 075021 (2010).
- [39] P. Ball and R. Zwicky, *J. High Energy Phys.* **10** (2001) 019.
- [40] P. Ball, *Phys. Lett. B* **644**, 38 (2007).
- [41] C. D. Lü, *Int. J. Mod. Phys. A* **23**, 3250 (2008).
- [42] J. Beringer *et al.* (Particle Data Group), *Phys. Rev. D* **86**, 010001 (2012).
- [43] G. Duplancic, A. Khodjamirian, T. Mannel, B. Meli, and N. Offen, *J. Phys. Conf. Ser.* **110**, 052026 (2008).
- [44] K. Abe *et al.* (Belle Collaboration), [arXiv:hep-ex/0410006v2](https://arxiv.org/abs/hep-ex/0410006v2).
- [45] H.-n. Li, Y.-L. Shen, Y.-M. Wang, and H. Zou, *Phys. Rev. D* **83**, 054029 (2011).